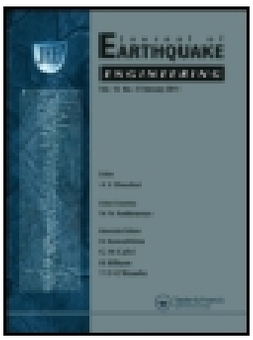

Taylor & Francis
Taylor & Francis Group

Journal of Earthquake Engineering

ISSN: 1363-2469 (Print) 1559-808X (Online) Journal homepage: http://www.tandfonline.com/loi/ueqe20

Effect of AAC Infill Walls on Structural System Dynamics of a Concrete Building

Professor Ozan Cem Celik

To cite this article: Professor Ozan Cem Celik (2015): Effect of AAC Infill Walls on Structural System Dynamics of a Concrete Building, Journal of Earthquake Engineering

To link to this article: http://dx.doi.org/10.1080/13632469.2015.1104757

Accepted author version posted online: 29 Oct 2015.

Effect of AAC Infill Walls on Structural System Dynamics of a Concrete Building

Professor Ozan Cem Celik

(Corresponding Author)

Email: occelik@metu.edu.tr

Middle East Technical University, Northern Cyprus Campus, Civil Engineering Program, Kalkanli, Guzelyurt, KKTC, Mersin, 10 Turkey

Abstract

The effect of autoclaved aerated concrete (AAC) infill walls on the structural system dynamics of a two-story reinforced concrete building is investigated using its finite element structural model, which is calibrated to simulate the acceleration-frequency response curves from its forced vibration test. The model incorporating the AAC infill walls by equivalent diagonal struts captures the increase in lateral stiffness of the building and the torsional motions induced due to the asymmetrically placed AAC infill walls. A higher strut width coefficient than in ASCE/SEI 41-06 is recommended to model the stiffness of the AAC infill walls in the elastic range.

Keywords: Buildings; dynamic properties; dynamic tests; field tests; masonry blocks; non-structural elements; struts; structural dynamics.

Introduction

Infill walls are usually not considered as part of the structural system in the design of buildings. Consequently, the effect of infill walls on the building mass and weight is considered, but their

effect on the stiffness and strength of the building is ignored in the structural analysis. This practice leads to good designs without a doubt only if the infill walls are properly isolated from the structural system such that their stiffness and strength do not affect the structural system behavior [Kaushik *et al.*, 2006; Sucuoglu, 2013; Mosalam and Gunay, 2014]. However, the common rationale behind this assumption in the structural analysis is that infill walls crack well below design level lateral loads and do not contribute to the stiffness of the building [Hashemi and Mosalam, 2007; Asteris *et al.*, 2011]. On the contrary, experimental and analytical studies on buildings with infill walls [Hashemi and Mosalam, 2007; Asteris *et al.*, 2013] and the earthquake performance of such buildings [Ricci *et al.*, 2011; Mosalam and Gunay, 2014] have long shown that infill walls increase the lateral stiffness of structural systems, reduce their fundamental periods, and often increase the seismic demand on them. Moreover, ignoring infill walls can result in weak stories, torsional irregularities, and short columns [Celarec *et al.*, 2012; Mosalam and Gunay, 2014]. Hence, infill walls have to be incorporated in the structural design process by isolating them from the structural system, preventing their adverse effects on the structural system [CEN, 2004], or including them in the finite element models.

Notwithstanding the large number of studies in the literature, there is still no consensus on how to model infill walls in a rational and practical manner [Asteris *et al.*, 2011; 2013]. On the experimental front [Hashemi and Mosalam, 2007; Asteris *et al.*, 2011; 2013; Soyoz *et al.*, 2013], quasi-static, pseudo-dynamic, and shake table tests, mostly on reduced-scale specimens, and ambient and forced vibration tests on existing buildings have been performed. Tests on full-scale specimens and existing buildings are particularly important. Penna *et al*. [2008] performed quasi-static cyclic tests on one-story one-bay reinforced concrete frames with autoclaved aerated

concrete (AAC) infill walls and determined that the lateral stiffness and strength of the frames were increased with respect to those of the reference bare frame. Ambient vibrations of buildings were recorded by a number of researchers before and after the infill walls were in place to evaluate their effect on the structural system dynamics. Chaker and Cherifati [1999] and Guler *et al*. [2008] respectively tested a three- and a twelve-story reinforced concrete moment frame with brick infill walls. Memari *et al*. [1999] performed ambient vibration tests on a six-story steel building with AAC interior walls and brick exterior walls, whereas Soyoz *et al*. [2013] tested a six-story reinforced concrete building retrofitted with cast-in-place reinforced concrete walls. Forced vibration tests were also performed on these buildings: Memari *et al*. [1999] when 50% of the walls were in place and Soyoz *et al*. [2013] when the seismic retrofit was completed. Forced vibration testing of existing buildings provides the most direct means of determining the structural system dynamic properties: natural vibration periods, natural modes of vibration, and modal damping capacities through well-established methods in the structural dynamics area [Celik *et al*., 2015], which do not require sophisticated system identification algorithms, and can reliably be used to determine the dynamic behavior of structural systems with infill walls in the elastic range. Note that forced vibrations are higher by orders of magnitude in amplitude than ambient vibrations. At all these tests, ambient or forced, natural vibration periods of buildings were reduced with the incorporation of the infill walls into the structural system. On the modeling front, simple strut models [Asteris *et al.*, 2011] to advanced continuum models [Asteris *et al*., 2013] have been proposed. The equivalent diagonal strut model proposed by Stafford Smith and Carter [1969] and later revised by Mainstone [1974] is the most adopted by

researchers and also adopted by the U.S. seismic rehabilitation provisions, ASCE/SEI 41-06 [ASCE, 2007].

This paper presents the effect of AAC infill walls on the structural system dynamics of a two-story reinforced concrete building through its finite element structural model calibrated with its forced vibration test [Celik, 2002]. A roof level vibration generator was used to excite the building and eight uniaxial accelerometers deployed throughout the floors recorded the structural vibrations. Torsional motions were measured due to the asymmetric layout of AAC infill walls in plan. Experimental acceleration-frequency response curves were simulated using the finite element model of the building that incorporated the infill walls by diagonal struts [ASCE, 2007]. The equivalent diagonal strut thickness was calibrated to match the experimental curves, and the related ASCE/SEI 41-06 equation was modified for predicting the response of structural systems with AAC infill walls in the elastic range. This study also adds to the very limited test data in the literature on the structural system dynamics of existing buildings with AAC infill walls, which have been increasingly used in recent years due to their light weight, ease of construction, and good insulation properties among others.

Forced vibration testing

Building description

New addition to the Structural Mechanics Lab of METU Civil Engineering Department is a two-story reinforced concrete building in Ankara, Turkey (see Fig. 1 for the front view). The ground

floor is 4.0 m and the first floor is 3.2 m high (centerline dimensions). The building is rectangular in plan, 6.3 m by 30.0 m, and has a single bay along the short axis and four bays along the long axis (Fig. 2). Columns are 400 by 400 mm and beams along the long axis are 360 by 550 mm, all cast-in-place (grade C25 concrete, for which TS 500 [Turkish Standards Institute, 2000] defines the characteristic compressive strength as 25 MPa). On the other hand, 400 by 650 mm beams along the short axis and 200 mm thick slab panels are all precast (grade C40 concrete). The structural system is symmetric in plan; however, infill walls made of AAC blocks distort this symmetry. Partition walls exist only on the left side of the ground floor, which is allocated for office use, whereas an open-space lab exists on the right side (Fig. 2c). On the first floor, partition walls are symmetrically placed along the short axis, but not along the long axis, due to the offices on the front side of the building (Fig. 2b). On-site measurements revealed that partition walls vary in thickness: those on the ground floor are 130 mm except that on axis 1.5, which is 200 mm; on the first floor those on axes 1.5 and 4.5 are 130 mm and that on axis A.7 is 140 mm, those elsewhere are 110 mm on average (varying between 80 and 140 mm). Exterior walls, on the other hand, are 200 mm thick. A first-floor skyway connects the building to the main lab building from the third bay at the backside of the building (B3-B4; Fig. 2b).

Instrumentation scheme

A vibration generator (Model VG-1 [Kinemetrics, 1975]; Fig. 3a) mounted on top of a beam-column joint at B3 on the roof (Fig. 2a) was used to excite the building with a horizontal unidirectional sinusoidal force (in kN):

$$p(t) = 0.43 f^2 \sin 2\pi f t \quad (1)$$

where f is the excitation frequency (in Hz) and t is the time (in s). Eight uniaxial accelerometers of force balance type (EpiSensor ES-U [Kinemetrics, 2000]) connected to a 12-channel digital recorder (K2 [Kinemetrics, 1997]; Fig. 3b) were used in recording the structural vibrations. Four accelerometers were mounted on the sides of each floor, two along the short axis and two along the long axis to extract the torsional responses, if any, as shown in Fig. 2 (see Fig. 3c for accelerometer #3).

Signal processing and frequency-response curves

Forced vibration test of the building was performed along its short and long axes, respectively. Lead weights that were placed in the buckets of the vibration generator (S1 loading [Kinemetrics, 1975]), which rotate in counter directions to produce the sinusoidal force in Eq. 1, limited the operating frequency to 7.2 Hz as the vibration generator was designed to produce a force up to 22 kN amplitude. Note that the maximum operating frequency is 9.7 Hz with empty baskets. Sweeping the frequency of the vibration generator from 0.5 to 7.0 Hz with increments of typically 0.05 Hz, the steady-state structural response of the building after the transient response damped out was recorded for 15 s from eight channels at each operated frequency. Sampling frequency of the accelerations, which was set to 200 Hz, comfortably satisfied the Nyquist frequency criterion. Band-pass filters were used to remove the DC offset and filter out the noise in the acceleration records, particularly when the frequency of the vibration generator was away from the resonant frequency of the building.

Plotting the response amplitudes at each frequency resulted in frequency-response curves in the form of acceleration amplitude versus excitation frequency [Rea *et al*., 1968] as shown in Fig. 4 for the excitation along the short and long axes of the building (note that line plots were determined through subsequent finite element simulations). These frequency-response curves were determined for a force with amplitude proportional to the square of the excitation frequency ω (= $2\pi f$; cf. Eq. 1). Measured responses can be divided by ω^2 and ω^4 to determine acceleration- and displacement-frequency response curves, respectively, for a constant-amplitude harmonic force.

Structural system dynamic properties

Natural vibration frequencies (periods) and modal damping capacities can be identified from any of the above frequency-response curves for the practical range of damping in structures [Chopra, 1995]. First mode natural frequency along the short axis was determined as 6.0 Hz (cf. Fig. 4a), i.e., the fundamental period was determined as 0.17 s. Accelerations recorded by accelerometers #2 and #6 were respectively higher than those by accelerometers #1 and #5 (Fig. 4a). Torsional motions induced were due to the asymmetric layout of the infill walls in the building, which otherwise has a symmetric structural system (Fig. 2). Note that the resonance acceleration was about 0.07 g. First mode damping capacity was calculated as 4.6% using the half-power bandwidth method [Rea *et al*., 1968; Chopra, 1995]. First mode shape determined from measured responses at the resonant frequency is presented subsequently.

It was not possible to excite the first mode along the long axis. Apparently, the associated natural frequency was higher than 7.0 Hz (cf. Fig. 4b). The test could be continued up to 9.7 Hz with empty baskets had it not stopped due to the loosening of one of the bolts that were used in mounting the vibration generator to the building. Dynamic structural properties along the long axis were not directly identified; however, frequency-response curves along the long axis were subsequently used in comparisons with the finite element simulations.

Finite element modeling

3-D linear elastic finite element structural model of the building was developed using SAP2000 [Computers and Structures, 2012] (Fig. 5). Frame elements were used to model the columns and beams. The moment of inertia of the beams was taken as two times that for the web. Slabs were assumed rigid in their own plane and rigid diaphragms were defined at all floors. All joints including the foundation-column joints were designated as moment connections in the design documents; therefore, fixed support conditions were used. Soil-structure interaction effects were ignored. Moduli of elasticity for grade C25 and C40 concrete were taken as 30,000 and 34,000 MPa, respectively [Turkish Standards Institute, 2000], whereas the unit weight of concrete was taken as 24 kN/m^3 in the structural model. Floor masses were calculated to be 190 and 160 tons for the first and second floors, respectively. Masses were lumped at the geometric center.

Infill modeling

The equivalent diagonal strut model [Stafford Smith and Carter, 1969; Mainstone, 1974] adopted by ASCE/SEI 41-06 was used in modeling all exterior and interior walls of the building, which were made of AAC blocks. The width of the equivalent strut, which represents the elastic in-plane stiffness of a solid infill panel prior to cracking, is given by

$$a = 0.175(\lambda h_c)^{-0.4} r_i \tag{2}$$

where $\lambda = \sqrt[4]{E_i t_i \sin 2\theta / 4 E_f I_c h_i}$; h_c and I_c are respectively the height (centerline dimension) and moment inertia of the column around the infill panel; r_i, t_i, and h_i are respectively the diagonal length, thickness, and height of the infill panel; E_i and E_f are the moduli of elasticity of the infill and frame material, respectively; and $\theta = \sin^{-1}(h_i / r_i)$. The thickness and modulus of elasticity of the equivalent strut are the same as those of the infill panel.

The equivalent strut widths for the exterior infill walls along the short and long axis were computed as 750 and 900 mm, respectively, which were 11-12% of the infill panel diagonal lengths. The strut widths for the interior partition walls, which were not surrounded by frames, were assumed to be 10% of the panel diagonal lengths due to lack of available formulation in the current state of the art. The modulus of elasticity for AAC blocks was taken as 2500 MPa based on an experimental study conducted at the Structural Mechanics Lab of METU Civil Engineering Department [Alakoc, 1999].

Window (2.0 × 1.6 m) and door (0.8 × 2.0 m) openings in infill walls result in reduced lateral stiffness as compared to solid walls [Asteris, 2003]. Such openings exist on the front side of the building (Fig. 1) and on the backside of the first floor of the building. All interior partition walls except those in between the offices on the first floor have door openings. The effect of these openings can be considered by a stiffness reduction factor, α, defined as a function of opening percentage, r_o (opening area/infill panel area) [Mosalam, 1996; Mondal and Jain, 2008; Asteris *et al*., 2013]. The equivalent strut width was reduced by

$$\alpha = 1 - 2r_o \tag{3}$$

in the presence of openings in this study, consistent with the findings of Mosalam [1996].

The stiffness reduction factors were computed as 0.5 for all exterior walls with openings. The only exceptions were those at the backside of the building on the first and last bays of the first floor, where there are single window openings, for which the reduction factors were computed as 0.7. On the other hand, they were computed as 0.8 and 0.7 for the partition walls with openings along the short and long axes, respectively.

Steady-state analysis

Natural vibration frequencies of the building from eigenvalue analysis of its finite element structural model can be compared with those identified from its forced vibration test [Celik *et al*., 2015]. The match can be misleading when there are a large number of uncertain parameters to be calibrated in the finite element model as several combinations of the values of these parameters

can lead to a similar result. Rather than merely comparing the modal properties, acceleration-frequency response curves were simulated through steady-state analysis [Computers and Structures, 2012] for comparison with the experimental curves in this study.

Modal damping ratio of 4.6% as determined from the forced vibration test was employed in the analysis. Note that modal damping can be approximated in frequency-domain analysis by using stiffness proportional hysteretic damping with coefficient twice the modal damping ratio [Computers and Structures, 2012].

The equivalent strut width coefficient 0.175 in Eq. 2 is the main parameter that was calibrated on a trial-and-error basis. Figure 4 shows the comparison of the experimental acceleration-frequency response curves with their analytical counterparts when the strut coefficient was taken as 0.38. The match is quite good and torsional motions induced due to the infill walls, which distort the structural system symmetry, were captured. Note that the comparison is not based on a single acceleration value measured at a particular frequency but on 280 individual acceleration-frequency measurements. Recently, Chrysostomou and Asteris [2012] also showed that Eq. 2 underestimates the stiffness of infill panels and recommended a higher strut coefficient 0.27.

The equivalent strut width is known to vary with applied loading [Stafford Smith and Carter, 1969]. Chrysostomou and Asteris [2012] used the equations by Stafford Smith and Carter [1969] and showed that the strut width to represent the initial stiffness of the infill panel is approximately twice the strut width at the onset of infill panel crushing (which is comparable to Eq. 2). Mehrabi *et al*. [1996] came up with a similar result earlier from an experimental study on reinforced concrete frames with masonry infill walls. These results justify the use of two

diagonal struts per infill panel in the elastic range in this study. Similarly, Sattar and Liel [2010] used twice the stiffness obtained from the equivalent strut width for modeling the initial stiffness of masonry infill panels.

Among other parameters calibrated were the mass moment of inertia about the vertical axis for each floor (respectively 17,000 and 13,000 $t \cdot m^2$ for the first and second floors) and the coefficient 2 in Eq. 3 to take into account the openings in infill walls. Fine-tuning of these parameters, which could result in an improved match between the experimental and simulated acceleration-frequency response curves in Fig. 4, was not sought as infill parameters have the greatest impact on dynamic response [Celarec *et al*., 2012].

Eigenvalue analysis

Eigenvalue analysis of the finite element structural model was also performed to present the natural vibration frequencies of the building that were not excited during its forced vibration test (cf. Table 1). The second mode is translational along the long axis of the building with a natural frequency of 7.9 Hz, whereas the third mode is torsional with a frequency of 8.7 Hz, which are beyond the frequency limit of the vibration generator when loaded with lead weights (cf. Sec. 2.3). Natural vibration frequencies of the bare frame (without the infill walls) are also presented in Table 1, which confirm that AAC infill walls increase the lateral stiffness of the building significantly.

First mode shape of the building along its short axis as determined from the finite element model is very well in agreement with the forced vibration test results as shown in Fig. 6.

Conclusions

The contribution of infill walls to the stiffness and strength of the structural system is usually overlooked in practice as they are considered as non-structural elements. On the contrary, recent experimental and analytical studies and their earthquake performance point to the need for incorporating the infill walls in the structural design process. To shed light on the behavior and structural modeling of buildings with infill walls in the elastic range, this paper investigated the effect of infill walls made of AAC blocks on the structural system dynamics of a two-story reinforced concrete building through finite element modeling and forced vibration testing. AAC infill walls increased the lateral stiffness of the building significantly. Translational vibration frequencies were 2–3 times higher than those of the bare frame. Asymmetrically placed infill walls in plan induced torsional motions during the forced vibration test of the building. The finite element structural model incorporating the AAC infill walls by equivalent diagonal struts was used to simulate the acceleration-frequency response curves through steady-state analysis rather than merely comparing the natural frequencies through eigenvalue analysis. The equivalent strut width coefficient in ASCE/SEI 41-06, which underestimated the stiffness of the AAC infill walls, was calibrated to match the experimental acceleration-frequency response curves. This study also added to the very limited test data in the literature on the structural system dynamics of existing buildings with AAC infill walls. Clearly, tests on full-scale specimens under large deformations and structural response monitoring of existing buildings during design level earthquake ground motions are needed to supplement the findings of this study.

References

Alakoc, C. A. [1999] "An experimental investigation on autoclaved aerated concrete (AAC) blocks and walls," M.Sc. thesis, Civil Engineering Department, Middle East Technical University, Ankara, Turkey.

ASCE [2007] Seismic Rehabilitation of Existing Buildings, ASCE standard ASCE/SEI 41-06, American Society of Civil Engineers, Reston, VA.

Asteris, P. G. [2003] "Lateral stiffness of brick masonry infilled plane frames," Journal of Structural Engineering 129(8), 1071–1079.

Asteris, P. G., Antoniou, S. T., Sophianopoulos, D. S., and Chrysostomou, C. Z. [2011] "Mathematical macromodeling of infilled frames: State of the art," Journal of Structural Engineering 137(12), 1508–1517.

Asteris, P. G., Cotsovos, D. M., Chrysostomou, C. Z., Mohebkhah, A., and Al-Chaar, G. K. [2013] "Mathematical micromodeling of infilled frames: State of the art," Engineering Structures 56, 1905–1921.

Celarec, D., Ricci, P., and Dolsek, M. [2012] "The sensitivity of seismic response parameters to the uncertain modeling variables of masonry-infilled reinforced concrete frames," Engineering Structures 35, 165–177.

Celik, O. C. [2002] "Forced vibration testing of existing reinforced concrete buildings," M.Sc. Thesis, Civil Engineering Department, Middle East Technical University, Ankara, Turkey.

Celik, O. C., Sucuoglu, H., and Akyuz, U. [2015] "Forced vibration testing and finite element modeling of a nine-story reinforced concrete flat plate-wall building," Earthquake Spectra 31(2), 1069–1081.

CEN [2004] Eurocode 8: Design of structures for earthquake resistance - Part 1: General rules, seismic actions and rules for buildings, European Standard EN 1998-1, European Committee for Standardization, Brussels, Belgium.

Chaker, A. A. and Cherifati, A. [1999] "Influence of masonry infill panels on the vibration and stiffness characteristics of R/C frame buildings," Earthquake Engineering and Structural Dynamics 28, 1061–1065.

Chopra, A. K. [1995] Dynamics of Structures, Prentice Hall, Upper Saddle River, NJ.

Chrysostomou, C. Z. and Asteris, P. G. [2012] "On the in-plane properties and capacities of infilled frames," Engineering Structures 41, 385–402.

Computers and Structures [2012] SAP2000 version 15.2.0, http://www.csiamerica.com/products/sap2000 [5 October 2014], Walnut Creek, CA.

Guler, K., Yuksel, E., and Kocak, A. [2008] "Estimation of the fundamental vibration period of existing RC buildings in Turkey utilizing ambient vibration records," Journal of Earthquake Engineering 12(S2), 140–150.

Hashemi, A. and Mosalam, K. M. [2007] "Seismic evaluation of reinforced concrete buildings including effects of masonry infill walls," PEER Report 2007/100, Pacific Earthquake Engineering Research Center, University of California, Berkeley, CA.

Kaushik, H. B., Rai, D. C., and Jain, S. K. [2006] "Code approaches to seismic design of masonry-infilled reinforced concrete frames: A state-of-the-art review," Earthquake Spectra 22(4), 961–983.

Kinemetrics [1975] Operating Instructions, Vibration Generator System, Model VG-1, San Gabriel, CA.

Kinemetrics [1997] Altus Digital Recorder User Manual, Pasadena, CA.

Kinemetrics [2000] EpiSensor Force Balance Accelerometer Model FBA ES-U User Guide, Document 301925, Pasadena, CA.

Mainstone, R. J. [1974] "Supplementary note on the stiffnesses and strengths of infilled frames," Current paper CP 13/74, Building Research Station, Garston, United Kingdom.

Mehrabi, A. B., Shing, P. B., Schuller, M. P., and Noland, J. L. [1996] "Experimental evaluation of masonry-infilled RC frames," Journal of Structural Engineering 122(3), 228–237.

Memari, A. M., Aghakouchak, A. A., Ashtiany, M. G., and Tiv, M. [1999] "Full-scale dynamic testing of a steel frame building during construction," Engineering Structures 21, 1115–1127.

Mondal, G. and Jain, S. K. [2008] "Lateral stiffness of masonry infilled reinforced concrete (RC) frames with central opening," Earthquake Spectra 24(3), 701–723.

Mosalam, K. M. [1996] "Modeling of the nonlinear seismic behavior of gravity load designed frames," Earthquake Spectra 12(3), 479–492.

Mosalam, K. M. and Gunay, S. [2014] "Progressive collapse analysis of RC frames with URM infill walls considering in-plane/out-of-plane interaction," Earthquake Spectra, in press.

Penna, A., Magenes, G., Calvi, G. M., and Costa, A. A. [2008] "Seismic performance of AAC infill and bearing walls with different reinforcement solutions," Proceedings of the 14th International Brick and Block Masonry Conference, Sydney, Australia.

Rea, D., Bouwkamp, J. G., and Clough, R. W. [1968] "Dynamic properties of McKinley school buildings," Report No. EERC 68-4, University of California, Berkeley, CA.

Ricci, P., Verderame, G. M., and Manfredi, G. [2011] "Analytical investigation of elastic period of infilled RC MRF buildings," Engineering Structures 33, 308–319.

Sattar, S. and Liel, A. B. [2010] "Seismic performance of reinforced concrete frame structures with and without masonry infill walls," Proceedings of the 9th US National and 10th Canadian Conference on Earthquake Engineering, Toronto, Canada.

Soyoz, S., Taciroglu, E., Orakcal, K., Nigbor, R., Skolnik, D., Lus, H., and Safak, E. [2013] "Ambient and forced vibration testing of reinforced concrete building before and after its seismic retrofitting," Journal of Structural Engineering 139(10), 1741–1752.

Stafford Smith, B. and Carter, C. [1969] "A method of analysis for infilled frames," ICE Proceedings 44(1), 31–48.

Sucuoglu, H. [2013] "Implications of masonry infill and partition damage in performance perception in residential buildings after a moderate earthquake," Earthquake Spectra 29(2), 661–667.

Turkish Standards Institute [2000] Requirements for Design and Construction of Reinforced Concrete Structures, TS 500, Ankara, Turkey.

Fig. 1. Front view of the building.

Fig. 2. Floor plans: (a) second (roof), (b) first, (c) ground; (d) Elevation; Instrumentation scheme.

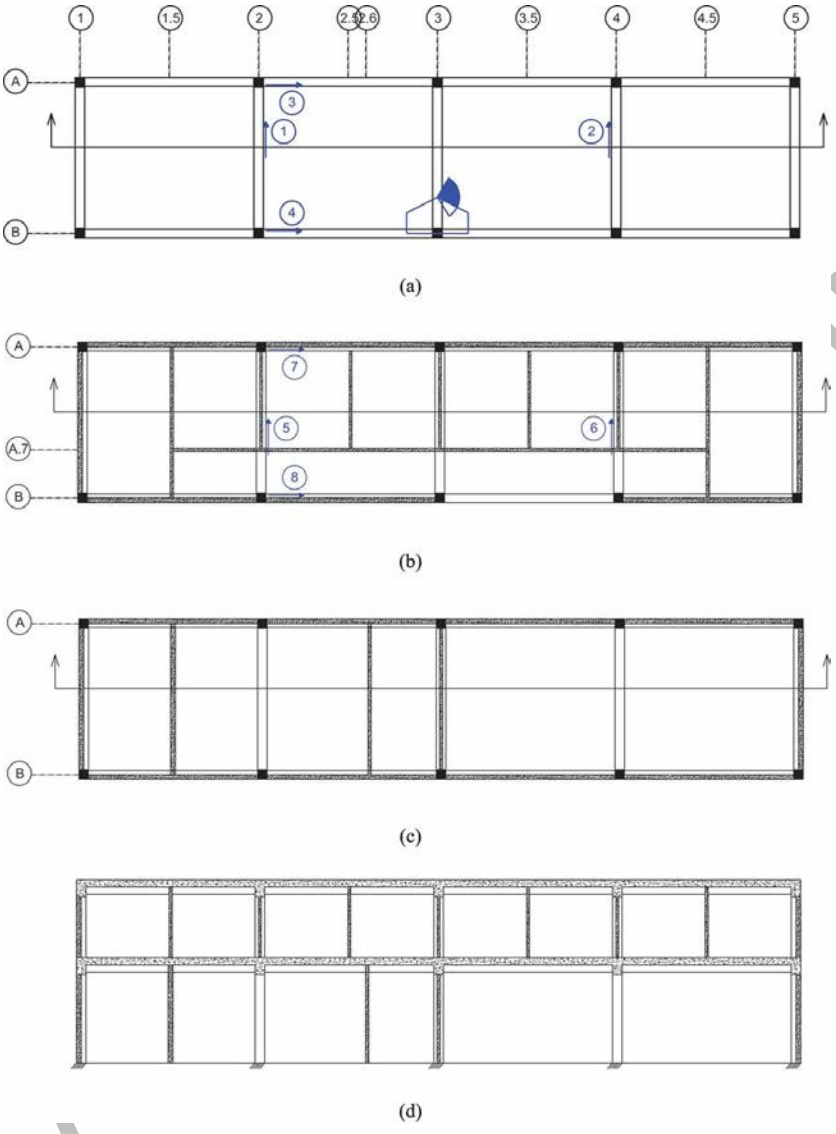

Fig. 3. (a) Vibration generator, (b) data acquisition system, (c) accelerometer #3.

(a)

(b) (c)

Fig. 4. Acceleration-frequency response curves for the excitation along (a) short and (b) long axes of the building.

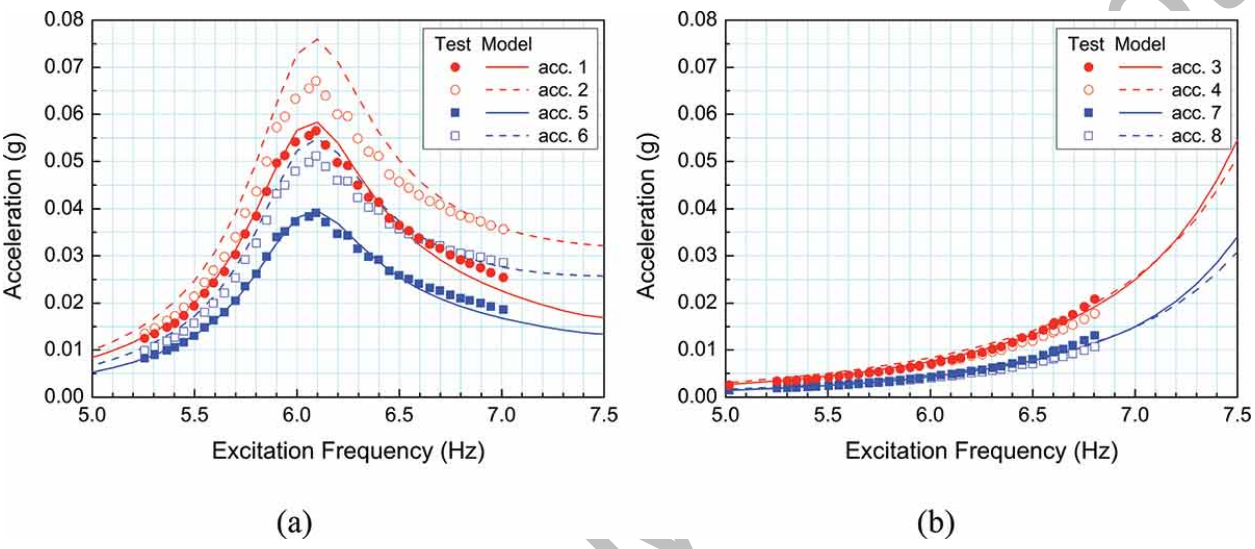

Fig. 5. 3-D finite element structural model.

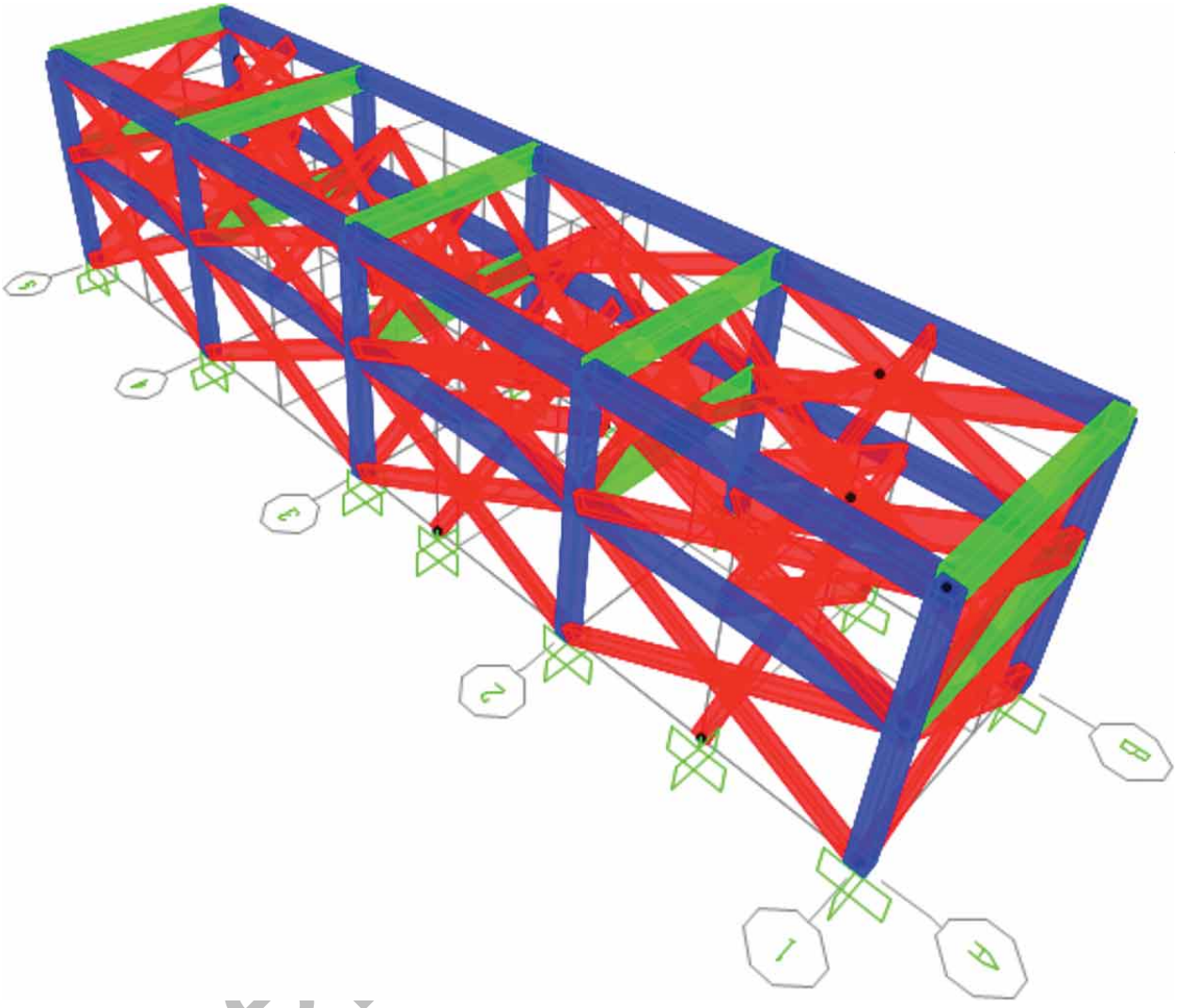

Fig. 6. First mode shape of the building along its short axis (arbitrary scale).

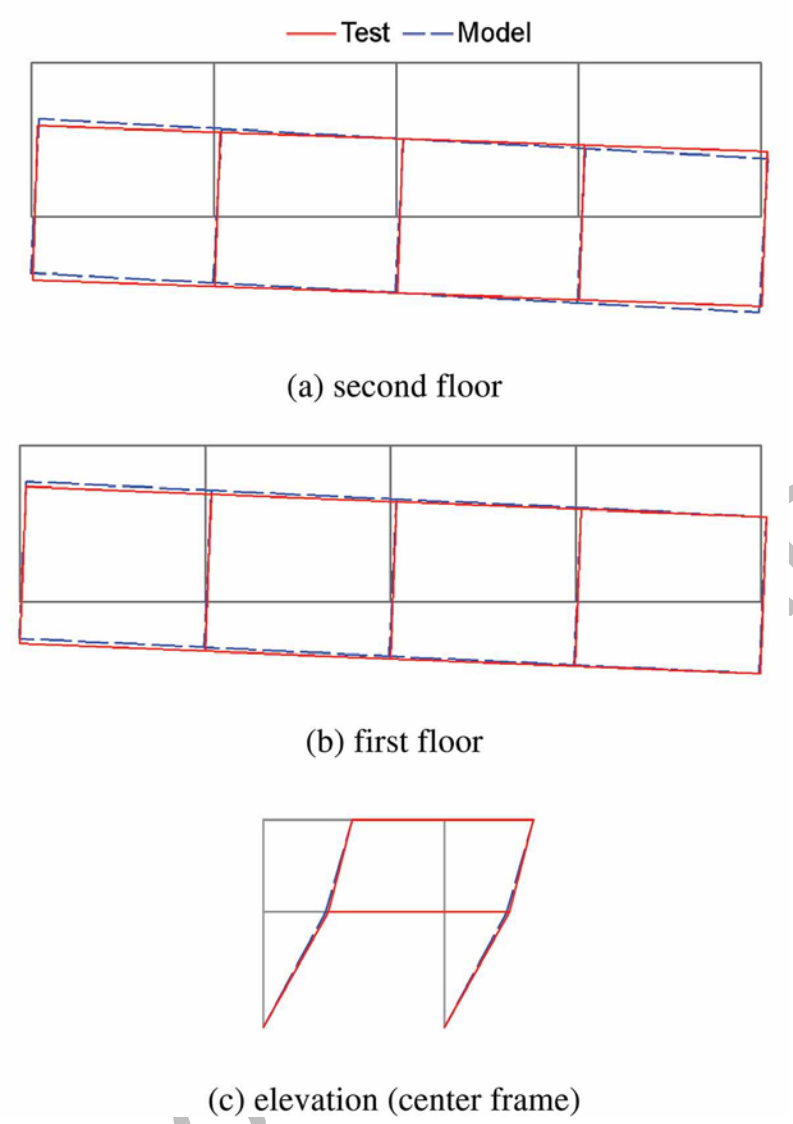

(a) second floor

(b) first floor

(c) elevation (center frame)

Table 1. Natural vibration frequencies of the building with and without the AAC infill walls.

	f **(Hz)**		
Mode	**w/ infill**	**w/o infill**	**Description**
1	6.0	2.5	Short axis translation
2	7.9	2.4	Long axis translation